Reactions of Monochloramine with Br_2, Br_3^-, HOBr, and OBr^-: Formation of Bromochloramines

Michael Gazda and Dale W. Margerum*

Department of Chemistry, Purdue University, West Lafayette, Indiana 47907

Received July 28, 1993®

Pulsed-accelerated-flow and stopped-flow spectroscopies are used to measure rate constants for the reactions of NH_2Cl with Br_2, Br_3^-, HOBr, and OBr^-: $NH_2Cl + Br_2 \xrightarrow{k_{Br_2}} NHBrCl + Br^- + H^+$; $NH_2Cl + Br_3^- \xrightarrow{k_{Br_3}} NHBrCl + 2Br^- + H^+$; $NH_2Cl + HOBr \xrightarrow{k_{HOBr}} NHBrCl + H_2O$; $NH_2Cl + OBr^- \xrightarrow{k_{OBr}} NHBrCl + OH^-$. Rate constants (25.0 °C) are $k_{Br_2} = (4.18 \pm 0.05) \times 10^8$ M^{-1} s^{-1}, $k_{Br_3} = (3.07 \pm 0.24) \times 10^7$ M^{-1} s^{-1}, $k_{HOBr} = (2.86 \pm 0.06) \times 10^5$ M^{-1} s^{-1}, and $k_{OBr} = (2.20 \pm 0.06) \times 10^4$ M^{-1} s^{-1}. In each reaction, nucleophilic attack of the nitrogen lone electron pair facilitates a Br^+ transfer from the bromine species to form the mixed haloamine NHBrCl, which decomposes slowly relative to its rate of formation. With the bromine species in excess, NBr_2Cl forms rapidly and subsequently decays with a half-life of ~5 min at pH 6.2. Aqueous molar absorptivities for NBr_2Cl are estimated as 4400 M^{-1} cm^{-1} at 242 nm and 550 M^{-1} cm^{-1} at 300 nm.

Introduction

Chlorination of ammoniacal waters leads to the formation of chloramines. Reactions of chloramines with various compounds in water systems are of environmental importance due to the widespread use of chlorine, hypochlorous acid, and chloramines in water treatment. Bromide ion may be present in water systems and it reacts with hypochlorous acid to give hypobromous acid.[1] Bromine compounds such as HOBr, Br_2, and BrCl are sometimes added directly to water systems for disinfection.[2] The active bromine compounds (Br_2, Br_3^-, HOBr and OBr^-) are also very good oxidizing agents in water systems.

Subsequent reactions of the chloramines with bromide ion and with the active bromine compounds are of interest in water treatment chemistry. The present work examines the kinetics, mechanisms, and products of the reactions of monochloramine (NH_2Cl) with the active bromine compounds.

Haag[3,4] proposed the formation of bromochloramine and dibromochloramine in the reaction of NH_2Cl with HOBr, as shown in eqs 1 and 2, and suggested that both NHBrCl and

$$NH_2Cl + HOBr \rightarrow NHBrCl + H_2O \quad (1)$$

$$NHBrCl + HOBr \rightarrow NBr_2Cl + H_2O \quad (2)$$

NBr_2Cl are important haloamines formed in the chlorination of seawater. Haag and Lietzke[5] predicted a rate constant of 5×10^3 M^{-1} s^{-1} for the reaction in eq 1. No other studies on the kinetics and mechanism of this reaction have been reported.

Gazda et al.[6] have provided molecular evidence that NHBrCl is the product of the reaction in eq 1. The second mixed haloamine, NBr_2Cl, has yet to be isolated and only an ether-extract UV–vis spectrum has been reported.[7] In the present work, an aqueous UV–vis spectrum is obtained for NBr_2Cl, and its decay rate at pH 6.2 is examined.

Experimental Section

Reagents. Distilled deionized water was used in all experiments. Bromine solutions were prepared by dissolving liquid Br_2 in dilute acid and were standardized spectrophotometrically. (Table 1 gives UV–vis spectral characteristics for species of interest.) Solutions of $HOBr/OBr^-$ that were free of bromide ion were prepared by mixing equimolar amounts of OCl^- and Br^- at pH ~ 9 (eq 3). Upon acidification to pH 3–6, no

$$OCl^- + Br^- \rightarrow OBr^- + Cl^- \quad (3)$$

Br_2 was detected in the resulting solution. This indicated the absence of bromide ion. The HOBr and OBr^- solutions were standardized spectrophotometrically. Hypochlorite ion solutions were prepared by dilution of a 10% NaOCl stock solution (Mallinckrodt) and standardized spectrophotometrically. Bromide ion solutions were prepared by dissolving solid NaBr in water and were standardized gravimetrically. Carbonate ion and phosphate ion buffers were prepared by dissolving their sodium salts in water. Sodium perchlorate solutions were prepared from recrystallized $NaClO_4$ and were standardized gravimetrically. Ammonia solutions were prepared by dilution of aqueous ammonia and were standardized by titration with standard HCl. Monochloramine solutions were prepared by mixing equimolar amounts of OCl^- and NH_3 and were standardized spectrophotometrically.

Methods. An Orion Model SA 720 Research digital pH meter equipped with a Corning combination electrode was used for pH measurements. The pH values were corrected to $p[H^+]$ values at 25.0 °C and $\mu = 0.50$ M based on electrode calibration by titration of standard $HClO_4$ with a standard NaOH solution.

A Perkin-Elmer Lambda 9 UV–vis–near-IR spectrophotometer interfaced to a Zenith 386/20 PC was used to obtain UV–vis spectra and to monitor the decomposition of NBr_2Cl. Extractions of nonionic and less polar species were carried out by mixing equal volumes of reactants in water with a T-mixer, followed by extraction of the reaction mixture into diethyl ether.

Reactions of NH_2Cl with HOBr and with OBr^- were monitored with a Durrum stopped-flow spectrophotometer interfaced to a Zenith 151 PC with a Metrabyte DASH-16 A/D interface card. The reactions were run under second-order unequal concentration conditions with $[NH_2Cl] = 1.85$ mM $= C_2$ and $[OBr^-]_T = 1.50$ mM $= C_1$. The loss of OBr^- was monitored at 400 nm (ϵ ~22 M^{-1} cm^{-1}) to avoid interferences from NH_2Cl and NHBrCl. All kinetic data gave good fits for initial absorbance (A_0), final absorbance (A_∞), and the second-order rate constant (k_r) as

* Abstract published in *Advance ACS Abstracts*, December 1, 1993.

(1) Kumar, K.; Margerum, D. W. *Inorg. Chem.* **1987**, *26*, 2706–2711.
(2) *Bromine Compounds: Chemistry and Applications;* Price, D., Iddon, B., Wakefield, B. J., Eds.; Elsevier: New York, 1988; pp 91–92.
(3) Haag, W. R. In *Water Chlorination: Environmental Impact and Health Effects*; Jolley, R. L., Brungs, W. A., Cumming, R. B., Jacobs, V. A., Eds.; Ann Arbor Science: Ann Arbor, MI, 1980; Vol. 3, pp 191–201.
(4) Haag, W. R. *J. Inorg. Nucl. Chem.* **1980**, *42*, 1123–1127.
(5) Haag, W. R.; Lietzke, M. H. In *Water Chlorination: Environmental Impact and Health Effects*; Jolley, R. L., Brungs, W. A., Cumming, R. B., Jacobs, V. A., Eds.; Ann Arbor Science: Ann Arbor, MI, 1980; Vol. 3, pp 415–426.
(6) Gazda, M.; Dejarme, L. E.; Choudhury, T. K.; Cooks, R. G.; Margerum, D. W. *Environ. Sci. Technol.* **1993**, *27*, 557–561.
(7) Haag, W. R.; Jolley, R. L. In *Water Chlorination: Environmental Impact and Health Effects*: Jolley, R. L., Brungs, W. A., Cotruvo, J. A., Cumming, R. B., Mattice, J. S., Jacobs, V. A., Eds.; Ann Arbor Science: Ann Arbor, MI; 1983; Vol. 4, pp 77–83.

0020-1669/94/1333-0118$04.50/0

Table 1. Maximum Absorbance Wavelengths and Molar Absorptivities in Water for Species of Interest

species	λ_{max}, nm	ϵ, M^{-1} cm^{-1}	ref
Br_2	390	173	*a*
Br_3^-	266	35000	*a*
HOBr	260	100	*a*
OBr^-	329	332	13
OCl^-	292	350	*a*
NH_2Cl	243	461	*b*
NHBrCl	220	2100	*c*
	320	300	*d*
NBr_2Cl	242	4400	this work

[a] Soulard, M.; Block, F.; Hatterer, A. *J. Chem. Soc., Dalton Trans.* **1981**, 2300–2310. [b] Kumar, K.; Day, R. A.; Margerum, D. W. *Inorg. Chem.* **1986**, *25*, 4344–4350. [c] Trofe, T. W.; Inman, G. W.; Johnson, J. D. *Environ. Sci. Technol.* **1980**, *14*, 544–549. [d] Valentine, R. L. *Environ. Sci. Technol.* **1986**, *20*, 166–170.

defined by eq 4, where A_t is the absorbance at a given time. Agreement

$$\ln\left[1 + \frac{C_2 - C_1}{C_1}\frac{A_0 - A_\infty}{A_t - A_\infty}\right] = \ln\frac{C_2}{C_1} + (C_2 - C_1)k_r t \quad (4)$$

with the second-order kinetic model confirms the rate law given in eq 5,

$$-\frac{d[OBr^-]_T}{dt} = k_r[NH_2Cl][OBr^-]_T \quad (5)$$

where $[OBr^-]_T = [OBr^-] + [HOBr]$. The solutions were buffered with carbonate ion or phosphate ion, and values for k_r were determined from p[H^+] 9.4 to p[H^+] 11.4. Ionic strength was maintained at 0.50 M with $NaClO_4$. All solutions were thermostated at 25.0 ± 0.1 °C.

Reactions of NH_2Cl with Br_2 and Br_3^- were monitored with a pulsed-accelerated-flow spectrophotometer (PAF),[8-10] Model IV.[10,11] The PAF method employs integrating observation during continuous flow mixing of short duration (a 0.22-s pulse). The reactants are observed along the direction of flow from their point of mixing to their exit from the observation tube (1.025 cm). A twin-path mixing/observation cell made of PVC is used. The flow was decelerated during the pulse to give a linear velocity ramp, and 250 measurements of the transmittance were taken as the flow velocity changed from 12 to 3 m s^{-1}. The velocity range is dictated by the need to have turbulent flow in the observation cell (>3 m s^{-1}) and by the pressure limitations of PAF IV (<12 m s^{-1}). Variation of the flow velocity permits the rate of the chemical reaction to be resolved from the rate of the mixing process. Solution reservoirs, drive syringes, and the mixing cell were thermostated at 25.0 ± 0.1 °C. Equation 6 was

$$M_{exp} = \frac{A_v - A_\infty}{A_0 - A_\infty} = \frac{1}{bk_m} + \frac{v}{bk_r'} \quad (6)$$

used in the analysis of PAF data under pseudo-first-order conditions, where M_{exp} is the defined absorbance ratio, A_v is the absorbance of the reaction mixture at a given instantaneous velocity, A_∞ is the absorbance after the reaction is complete, A_0 is the absorbance at time zero, k_r' is the reaction rate constant (s^{-1}), b is the reaction path length, v is the solution velocity in the observation tube (m s^{-1}), and k_m is a proportionality constant from the mixing rate constant (k_{mix}), where $k_m = k_{mix}/v$. Linear plots of M_{exp} vs v (M plots) have slopes of $1/(bk_r')$ for first-order reactions.

In the experiments, initial post-mixing conditions were $[NH_2Cl]$ = 0.10 mM, $[Br_2]_T = [Br_2] + [Br_3^-]$ = 0.01 mM, p[H^+] ~6.2, and bromide ion was varied from 0.075 to 0.200 M. All kinetic data were obtained by following the loss of Br_3^- at 266 nm. The rate constants reported are averages of four to six trials, and the values in parentheses denote 1 standard deviation in the last digit. Agreement with the first-order kinetic model confirms the rate law given in eq 7.

$$-\frac{d[Br_2]_T}{dt} = k_r'[Br_2]_T \quad (7)$$

Light Scattering Corrections for the PAF. Initial PAF experiments produced erratic results due to very large scattering effects caused by differences in the refractive indices of the reactants at 266 nm. The ionic strength of each solution was 0.50 M; however, the ionic strength in the NH_2Cl solution was maintained with $NaClO_4$, while the bromine solution contained both $NaClO_4$ and NaBr. In the PAF method, the reactant solutions are observed as they mix in turbulent flow. Differences in the refractive index of the solutions will cause schlieren patterns. Total reflectance can occur when the light beam strikes the interface of unmixed layers of solution at an angle greater than the critical angle.[12] The resultant light scattering causes a decrease in transmittance. The higher the flow velocity the greater the turbulence and the better the mixing which reduces the light scattering. This effect has been reported previously for PAF IV experiments, where scattering effects were small and could be effectively subtracted from the data.[13,14] In the present experiment the scattering effects associated with the high bromide ion concentration in the UV region were of such magnitude that the subtractive algorithm[15] was ineffective.

To solve this problem, calibration curves were constructed for the scattering effects of $NaClO_4$ and NaBr solutions. PAF absorbance signals were observed for varying concentrations of the solutions when they were mixed with water. Plots of the change in absorbance over the full range of flow velocites ($\Delta A_v = A_v$(3 m s^{-1}) - A_v(12 m s^{-1})) vs concentration for each reagent are shown in Figure 1 The NH_2Cl reactions were then run by matching the ΔA_v values for each compound. For example, if the bromine solution contained 0.075 M bromide ion, then the NH_2Cl solution would contain 0.125 M $NaClO_4$. These two solutions would produce the same ΔA_v, thus eliminating the light scattering. The ionic strengths of the mixed solutions were not exactly the same in each case, but the rate constants for these reactions are not affected by ionic strength because there is one neutral reactant.[16] Figure 2 shows an example of a PAF medium vs reactant file (a) without and (b) with scatter correction. In part a, the solutions are 0.01 mM $(Br_2)_T$/0.1 M NaBr/0.4 M $NaClO_4$ vs 0.5 M $NaClO_4$, and in part b, the solutions are 0.01 mM $(Br_2)_T$/0.1 M NaBr vs 0.275 M $NaClO_4$. The ΔA_v value decreased from 0.022 to essentially zero. A ΔA_v value of 0.022 is significant because, in these experiments, typical ΔA_v values for the reaction data were between 0.015 and 0.022. This method was successful in eliminating the scattering effect. Figure 2a also shows that, in the higher velocity region, where turbulence is higher and mixing is more efficient, the scattering effect is reduced. Conversely, mixing is not as efficient in the lower velocity region, where the light scattering is more pronounced.

Results and Discussion

Stoichiometry. In excess NH_2Cl, the reactions of NH_2Cl with the bromine compounds give a stoichiometric transfer of a bromine(I) cation (Br^+) to NH_2Cl to give the product, NHBrCl. This compound, however, decomposes in base to regenerate OBr^- as a final product. The overall process shown in eq 8 was proposed

$$2NHBrCl + OH^- \rightarrow N_2 + 3H^+ + 2Cl^- + Br^- + OBr^- \quad (8)$$

by Valentine[17] and is based on stoichiometries proposed by Cromer et al.[18] for the base decomposition of $NHBr_2$. If the reformation of OBr^- is a faster process than the reaction of NH_2Cl with OBr^-, the stoichiometry for the NH_2Cl/OBr^- reaction would be 2:1. If not, then the stoichiometry remains 1:1. To test this, NH_2Cl and OBr^- were mixed at a 1.3:1 mole ratio at the highest experimental p[H^+] (11.36), and the resulting reaction mixture was pushed

(8) Jacobs, S. A.; Nemeth, M. T.; Kramer, G. W.; Ridley, T. Y.; Margerum, D. W. *Anal. Chem.* **1984**, *56*, 1058–1065.
(9) Nemeth, M. T.; Fogelman, K. D.; Ridley, T. Y.; Margerum, D. W. *Anal. Chem.* **1987**, *59*, 283–291.
(10) Fogelman, K. D.; Walker, D. M.; Margerum, D. W. *Inorg. Chem.* **1989**, *28*, 986–993.
(11) Bowers, C. P.; Fogelman, K. D.; Nagy, J. C.; Ridley, T. Y.; Wang, Y. L.; Evetts, S. W.; Margerum, D. W. To be submitted for publication.
(12) Strobel, H. A.; Heineman, W. R. *Chemical Instrumentation: A Systematic Approach*, 3rd ed.; Wiley & Sons: New York, 1989; p 208.
(13) Troy, R. C.; Margerum, D. W. *Inorg. Chem.* **1991**, *30*, 3538–3543.
(14) Troy, R. C.; Kelley, M. D.; Nagy, J. C.; Margerum, D. W. *Inorg. Chem.* **1991**, *30*, 4845–4851.
(15) Dickson, P. N. Ph.D. Thesis, Purdue University, 1986.
(16) Espenson, J. H. In *Chemical Kinetics and Reaction Mechanisms;* McGraw Hill: New York, 1981; p 172.
(17) Valentine, R. L. Ph.D. Thesis, UC-Berkeley, 1983.
(18) Cromer, J. L.; Inman, G. W.; Johnson, J. D. In *Chemistry of Wastewater Technology*; Rubin, A. J., Ed.; Ann Arbor Science: Ann Arbor, MI, 1978; pp 213–225.

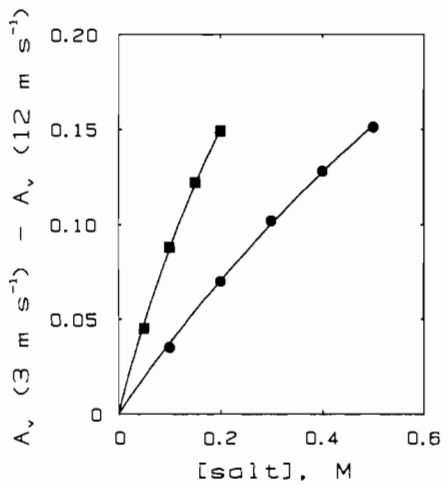

Figure 1. Light scattering effects of ionic medium for the pulsed-accelerated flow when salt solutions are mixed with water, showing dependence of ΔA_v (A_v(3 m s^{-1} flow velocity) - A_v (12 m s^{-1} flow velocity)) on $NaClO_4$ (circles) and NaBr (squares) concentrations on the PAF. Conditions: 25.0 ± 0.1 °C; monitoring at 266 nm.

Table 2. Stopped-Flow Data[a] for the Reactions of NH_2Cl with HOBr and with OBr^-

p[H^+]	buffer	$10^{-4}k_r$, M^{-1} s^{-1}
11.36	HPO_4^{2-}/PO_4^{3-}	2.3(3)
11.18		2.3(2)
10.47	HCO_3^-/CO_3^{2-}	2.6(3)
10.20		3.3(2)
9.93		4.2(2)
9.67		5.3(4)
9.42		7.3(5)

[a] Conditions: $[NH_2Cl]$ = 1.85 mM; $[OBr^-]_T$ = 1.5 mM; $[Buffer]_T$ = 25 mM; 25.0 ± 0.1 °C; μ = 0.50 M (with $NaClO_4$); monitoring the loss of OBr^- at 400 nm.

directly into ether for extraction. The resulting UV–vis spectrum in ether showed peaks at 220 nm and at 330 nm, indicative of NHBrCl.[6] This shows that the decomposition of NHBrCl (eq 8) is much slower than the reaction of NH_2Cl with OBr^- at this pH. Thus, a 1:1 stoichiometry is appropriate for the reaction between NH_2Cl and OBr^-.

Stopped-Flow Studies of the NH_2Cl Reactions with HOBr and with OBr^-. The reactions of NH_2Cl with HOBr and with OBr^- were studied as a function of p[H^+] by stopped-flow spectrophotometry. Under our experimental conditions, the concentrations of Br_2 and Br_3^- are negligible. We propose the mechanism given in eqs 9–11, where HA is either HCO_3^- or HPO_4^{2-}. The

$$OBr^- + NH_2Cl \xrightarrow{k_{OBr}} NHBrCl + OH^- \quad (9)$$

$$OBr^- + HA \rightleftharpoons HOBr + A^- \quad (10)$$

$$HOBr + NH_2Cl \xrightarrow{k_{HOBr}} NHBrCl + H_2O \quad (11)$$

buffer is needed to ensure rapid proton transfer to OBr^- to form HOBr. By solving the rate expression in eq 5 in terms of $[OBr^-]_T$ and $[HA]_T$, we obtain the expression in eq 12 for k_r, where K_{HOBr}

$$k_r = \frac{k_{OBr} + k_{HOBr}K_{HOBr}[H^+]}{1 + K_{HOBr}[H^+]} \quad (12)$$

= $[HOBr]/[OBr^-][H^+] = 10^{8.8}$ M^{-1}.[13] Table 2 summarizes the data and conditions for the stopped-flow experiments. Figure 3 shows a plot of the data and a smooth curve based on a best-fit of the data to eq 12 is included for comparison. Rate constants determined

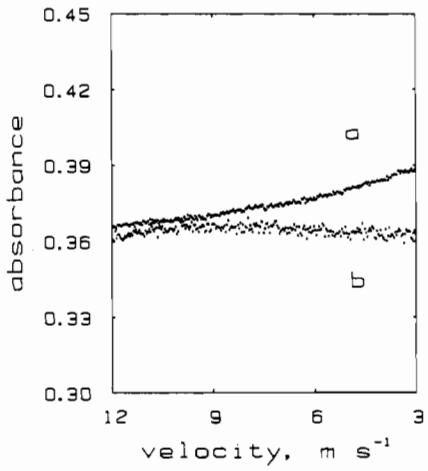

Figure 2. Example of a PAF medium vs reactant data file (a) without, and (b) with matching solutions to minimize light scattering based on the data in Figure 1. In part a, the solutions are 0.01 mM $(Br_2)_T$/0.1 M NaBr/0.4 M $NaClO_4$ vs 0.5 M $NaClO_4$, and in part b, the solutions are 0.01 mM $(Br_2)_T$/0.1 M NaBr vs 0.275 M $NaClO_4$. The ΔA_v value decreased from 0.022 to nearly zero.

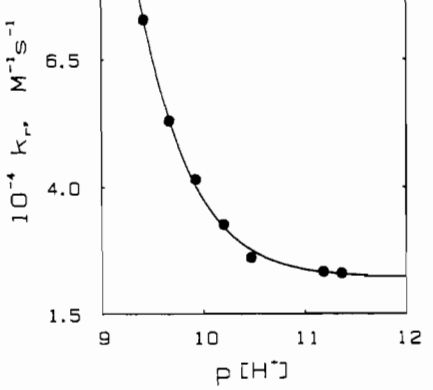

Figure 3. Dependence of the observed second-order rate constant on p[H^+] for the reactions of NH_2Cl with HOBr and with OBr^-. The curve is based on a fit of eq 12 where k_{OBr} = (2.20 ± 0.06) × 10^4 M^{-1} s^{-1} and k_{HOBr} = (2.86 ± 0.06) × 10^5 M^{-1} s^{-1}. Data and conditions are summarized in Table 2.

are k_{OBr} = (2.20 ± 0.06) × 10^4 M^{-1} s^{-1} and k_{HOBr} = (2.86 ± 0.06) × 10^5 M^{-1} s^{-1}. The rate constant for the HOBr reaction with NH_2Cl is similar to the rate constant for the reaction of HOBr with Br^- (2.24 × 10^5 M^{-1} s^{-1}).[19] The rate constants for the HOBr reactions may be correlated with the nucleophilicity of NH_2Cl and Br^- by the Swain–Scott relationship (eq 13),[20] where n is the

$$\log(k/k_o) = sn \quad (13)$$

nucleophilicity and s is the sensitivity of the reaction site. The nucleophilicity of NH_2Cl has not been reported, but can be estimated from the nucleophilicity of Br^- (n = 3.89).[21] By division of eq 14 by eq 15, n_{NH_2Cl} can be calculated as 3.97. (The reaction site is the bromine atom in HOBr in both cases, so the s values are the same.)

$$\log(k_{NH_2Cl}/k_0) = sn_{NH_2Cl} \quad (14)$$

$$\log(k_{Br^-}/k_0) = sn_{Br^-} \quad (15)$$

(19) Eigen, M.; Kustin, K. *J. Am. Chem. Soc.* **1962**, *84*, 1355–1361.
(20) Swain, C. G.; Scott, C. B. *J. Am. Chem. Soc.* **1953**, *75*, 141–147.
(21) Hine, J. *Physical Organic Chemistry;* McGraw-Hill: New York, 1962; p 161.

Another comparison that can be made with other nucleophiles is the ratio of the rate constants: k_{HOBr}/k_{OBr^-}. The ratios for several nucleophiles are as follows: for I^-, 7400;[13] for CN^-, 74;[22] for SO_3^{2-}, 50;[13] for NH_2Cl, 12. The value for NH_2Cl is the smallest, though of the same order of magnitude as those for CN^- and SO_3^{2-}. The ratio for NH_2Cl was expected to be larger because in the reactions of CN^-, I^-, and SO_3^{2-} with HOBr, the k_{HOBr} values are near the diffusion limit. This leads to the possibility that the reaction may be described by eq 16 rather than by eq 9. The reactions in eqs 9 and 16, however, are kinetically indistinguishable.

$$HOBr + NH_2Cl + OH^- \rightarrow NHBrCl + H_2O + OH^- \quad (16)$$

Structure I shows a transition state proposed for the reaction in eq 11; we propose nucleophilic attack at the bromine atom by the lone electron pair on the nitrogen. This yields a transfer of

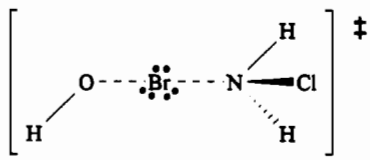

I

Br^+ to the nitrogen. The breakup of this transition state is followed by a fast proton transfer, as shown in eq 17.

$$I \rightarrow OH^- + NH_2BrCl^+ \rightarrow NHBrCl + H_2O \quad (17)$$

Transition states for the reactions in eqs 9 (with solvent assistance shown) and 16 are also proposed and are shown as

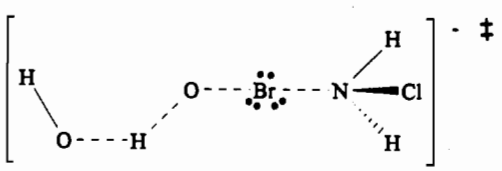

II

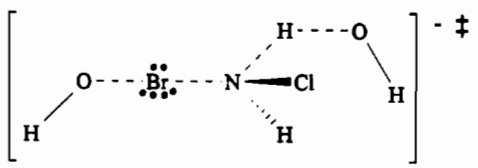

III

structures II and III, respectively. The transition states for eqs 9 and 16 would break up into products following the fast, subsequent steps shown in eqs 18 and 19.

$$II \rightarrow 2OH^- + NH_2BrCl^+ \rightarrow NHBrCl + H_2O + OH^- \quad (18)$$

$$III \rightarrow OH^- + NHBrCl + H_2O \quad (19)$$

Pulsed-Accelerated-Flow Studies of the NH_2Cl Reactions with Br_2 and with Br_3^-. The mechanism proposed at high bromide ion concentration in neutral to acidic solutions is shown in eqs 20–22. Under these conditions, the HOBr and OBr^- concentrations are negligible. The rate law for the loss of $[Br_2]_T$ is given in eq 7, and the expression for k_r', the pseudo-first-order rate constant, is given in eq 23.

(22) Gerritsen, C. M.; Gazda, M.; Margerum, D. W. *Inorg. Chem.*, in press.

$$Br_2 + Br^- \overset{K_{Br_3}}{\rightleftharpoons} Br_3^- \quad (20)$$

$$NH_2Cl + Br_2 \overset{k_{Br_2}}{\rightarrow} NHBrCl + Br^- + H^+ \quad (21)$$

$$NH_2Cl + Br_3^- \overset{k_{Br_3}}{\rightarrow} NHBrCl + 2Br^- + H^+ \quad (22)$$

$$k_r' = \left[\frac{k_{Br_2} + k_{Br_3}K_{Br_3}[Br^-]}{1 + K_{Br_3}[Br^-]}\right][NH_2Cl] \quad (23)$$

The reaction of NH_2Cl with Br_2 and with Br_3^- was examined with the PAF spectrophotometer under conditions to minimize light scattering. A typical M plot is shown in Figure 4. Figure

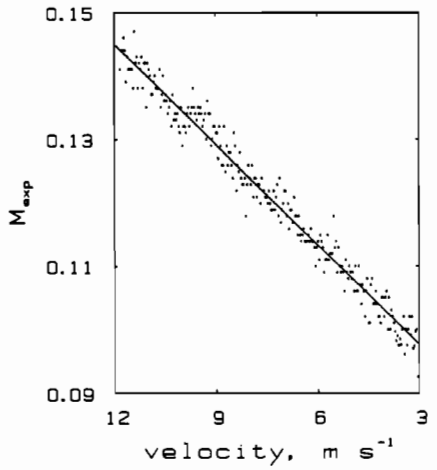

Figure 4. Experimental data for the reactions of NH_2Cl with Br_2 and with Br_3^- obtained by the pulsed-accelerated-flow method. M_{exp} is defined in eq 6, with $k_r' = -1/b(\text{slope}) = (1.85 \pm 0.02) \times 10^4\ s^{-1}$. The solid line is a least-squares fit.

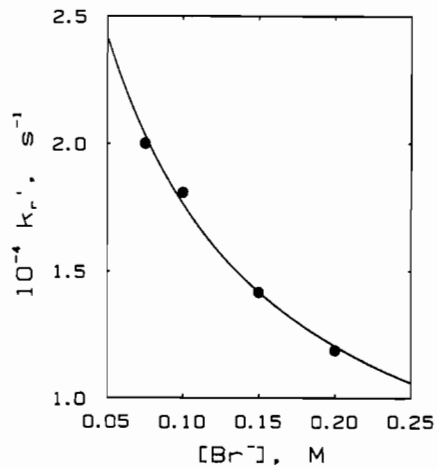

Figure 5. Dependence of the observed pseudo-first-order rate constant on $[Br^-]$ for the reactions of NH_2Cl with Br_2 and with Br_3^-. The curve is evaluated from eq 23 where $k_{Br_2} = (4.18 \pm 0.05) \times 10^8\ M^{-1}\ s^{-1}$ and $k_{Br_3} = (3.07 \pm 0.24) \times 10^7\ M^{-1}\ s^{-1}$. Data and conditions are summarized in Table 3.

5 shows the data and the best-fit of the data to eq 23. Table 3 summarizes the experimental conditions used and the rate constants obtained by the PAF method. Values determined for the Br_2 and Br_3^- rate constants are $(4.18 \pm 0.05) \times 10^8$ and $(3.07 \pm 0.24) \times 10^7\ M^{-1}\ s^{-1}$, respectively.

Transition states are proposed in structures IV and V, where a Br^+ transfer is again proposed via nucleophilic attack of the

Table 3. Pulsed-Accelerated-Flow Data[a] for the Reactions of NH_2Cl with Br_2 and with Br_3^-

[NaBr], M	[$NaClO_4$], M	μ, M	$10^{-4}k_r'$, s^{-1}
0.075	0.125	0.242	2.00(5)
0.100	0.275	0.417	1.81(6)
0.150	0.383	0.575	1.42(4)
0.200	0.490	0.732	1.19(2)

[a] Conditions: $[NH_2Cl] = 0.10$ mM; $[Br_2]_T = 0.01$ mM; $[phosphate]_T = 25$ mM; $p[H^+] \sim 6.2$; 25.0 ● 0.1 °C; monitoring the loss of Br_3^- at 266 nm.

Scheme 1

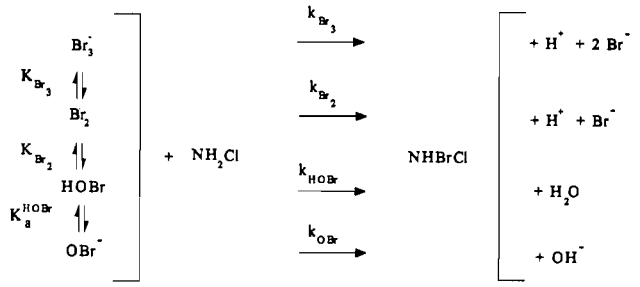

nitrogen lone pair on the bromine atom. These transition states would then break up to give NHBrCl, H^+, and Br^-.

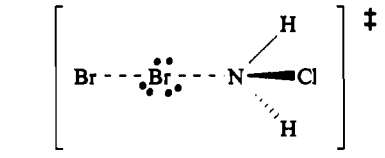

IV

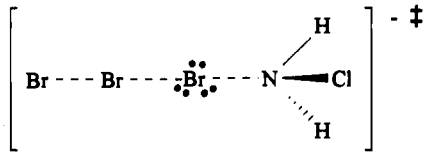

V

Overall Mechanism. An overall mechanism proposed for the reactions of NH_2Cl with Br_2, Br_3^-, HOBr and OBr^- is shown in Scheme I, with the rate law and the expression for k_{obsd} given in eqs 24 and 25. Figure 6 summarizes the behavior of the system

$$\frac{d[NHBrCl]}{dt} = k_{obsd}[NH_2Cl][Br_2]_T \quad (24)$$

$$k_{obsd} = (k_{Br_2}[Br^-][H^+]^2 + k_{HOBr}K_{Br_2}[H^+] + k_{OBr}K_a^{HOBr}K_{Br_2} + k_{Br_3}K_{Br_3}[Br^-]^2[H^+]^2)/([Br^-][H^+]^2 + K_{Br_2}[H^+] + K_a^{HOBr}K_{Br_2} + K_{Br_3}[Br^-]^2[H^+]^2) \quad (25)$$

calculated at three different bromide ion concentrations as a function of $p[H^+]$. The plot shows that all reactions are very fast, but that the rate constants vary by more than 4 orders of magnitude. Bromide ion concentration can significantly effect the observed rate constant, particularly in the neutral pH region. The conditions for curve a best describe those found in water treatment. Table 4 gives the values of the rate and equilibria constants for the expression in eq 25.

Reaction of NH_2Cl with Excess HOBr. In excess HOBr, Haag and Jolley[7] proposed the formation of NBr_2Cl (eqs 1 and 2) with aqueous spectral characteristics predicted as $\lambda_{max} \sim 240$ nm and $\epsilon_{240} \sim 6000$ M^{-1} cm^{-1}. We obtained the UV–vis spectra shown in Figure 7 upon mixing aqueous solutions of 1 mM NH_2Cl with 2 mM HOBr at pH 6.2. The compound formed has absorption

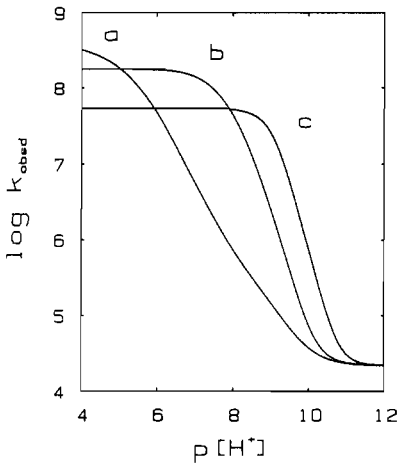

Figure 6. Dependence of the log of the observed second-order rate constant on $p[H^+]$ at (a) $[Br^-] = [OBr^-]$ above $p[H^+]$ 10 and $[Br^-] = 0$ M in acid (i.e., no added bromide ion), (b) $[Br^-] = 0.1$ M, and (c) $[Br^-] = 1.0$ M for the reactions of NH_2Cl with Br_2, Br_3^-, HOBr, and OBr^-. The expression for k_{obsd} is given in eq 25 and Table 4 summarizes the rate and equilibria constants.

Table 4. Summary of Rate and Equilibria Constants for Equation 25

const	value[a]
K_{Br_3}	16.6 M^{-1} [b]
K_{Br_2}	7.4×10^{-9} M^2 [c]
K_a^{HOBr}	1.58×10^{-9} M[d]
k_{Br_2}	$(4.18 \pm 0.05) \times 10^8$ M^{-1} s^{-1}
k_{Br_3}	$(3.07 \pm 0.24) \times 10^7$ M^{-1} s^{-1}
k_{HOBr}	$(2.86 \bullet 0.06) \times 10^5$ M^{-1} s^{-1}
k_{OBr}	$(2.20 \pm 0.06) \times 10^4$ M^{-1} s^{-1}

[a] 25.0 °C; $\mu = 0.50$ M. [b] Irving, H.; Wilson, P. D. *J. Inorg. Nucl. Chem.* **1964**, *26*, 2235–2239. [c] Wang, T. X.; Margerum, D. W. To be submitted for publication. [d] Reference 13.

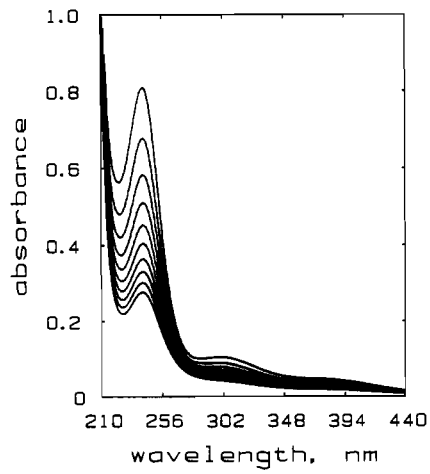

Figure 7. Aqueous UV–vis spectra showing the decay of NBr_2Cl. Conditions: $[NH_2Cl]_i = 0.46$ mM; $[HOBr]_i = 1.0$ mM; $[phosphate]_T = 25$ mM; $p[H^+] = 6.2$; 25.0 ± 0.1 °C; 1-min intervals between scans.

peaks at 242 and 300 nm and is assumed to be NBr_2Cl. Its decay follows a second-order dependence with an initial half-life of ~5 min. The second-order decay of NBr_2Cl indicates that if it is formed at low concentrations in water systems ($\sim 10^{-5}$–10^{-6} M), the compound would persist for significant periods of time. Aqueous molar absorptivities for NBr_2Cl are estimated as 4400 M^{-1} cm^{-1} at 242 nm and 550 M^{-1} cm^{-1} at 300 nm by extrapolating the decay curve to time zero and assuming complete conversion of NH_2Cl.

Upon addition of bromide ion (10–200 mM) to the excess HOBr, the resulting NBr_2Cl solutions were more stable than in the absence of Br^-. Ether extract UV–vis spectra of these solutions

showed that the NBr_2Cl concentration decreased as the Br^- concentration increased. The primary bromine (I) species in the presence of high Br^- concentration is Br_2. Thus, the reaction shown in eq 26 is proposed to be reversible. The decay rates of

$$NHBrCl + Br_2 \overset{K_1}{\rightleftharpoons} NBr_2Cl + Br^- + H^+ \qquad (26)$$

the haloamines and the overlapping spectra of the compounds make the value of K_1 difficult to determine. Monochloramine was not detected in any of the UV–vis spectra, indicating that the reaction of NH_2Cl with Br_2 is not reversible under these conditions.

Comparison of the Reactivities of Bromine Species. Bromine oxidation of $Co^{II}(edta)^{2-}$ is one of the few other systems where the relative reactivity of the four aqueous bromine species is known.[23] The relative reactivities given by the resolved rate constants ($M^{-1}\ s^{-1}$ at 25.0 °C) for the cobalt oxidation reactions are: OBr^- (2×10^3) $\gg$ HOBr (65) $\gg$ Br_2 (7.3×10^{-2}) $\simeq$ Br_3^- (5.4×10^{-2}). The initial product from the Br_2 and Br_3^- reactions is $Co^{III}(edta)Br^{2-}$, while the initial product from the HOBr and OBr^- reactions is $Co^{III}(edta)(H_2O)^-$. An inner-sphere electron-transfer mechanism was proposed[23,24] for the cobalt oxidation as opposed to the Br^+-transfer mechanism that we propose for the NH_2Cl reactions. The relative reactivities of the bromine species are very different for these two systems. The ratio of rate constants for Br_2/OBr^- is 3.6×10^{-5} for the $Co^{II}(edta)^{2-}$ reactions compared to 1.9×10^4 for the NH_2Cl reactions.

Other non-metal redox studies[13,22] where Br^+ transfer occurs to I^-, SO_3^{2-}, and CN^- also show a greater reactivity for HOBr compared to OBr^-. This is also the case for the reaction with ammonia to form bromamine.[25]

Conclusions

Pulsed-accelerated-flow and stopped-flow spectroscopies are used to measure the rapid reactions of NH_2Cl with Br_2, Br_3^-, HOBr, and OBr^-. These reactions all proceed by Br^+ transfer to yield NHBrCl as a product. The reaction rate constants vary by more than 4 orders of magnitude, with relative reactivies Br_2 > Br_3^- $\gg$ HOBr > OBr^-. The rate constant for the reaction of HOBr with NH_2Cl is similar to the rate constant for the reaction of HOBr with bromide ion. Therefore, the nucleophilicities of NH_2Cl and Br^- are similar when reacting with HOBr. With the bromine species in excess over NH_2Cl, NBr_2Cl readily forms and is moderately stable in neutral solutions. This work further establishes that bromochloramines are significant products in the chlorination of bromide-containing ammoniacal water systems.

Acknowledgment. This work was supported by National Science Foundation Grant CHE-9024291. M.G. also thanks the Procter & Gamble Co. for a fellowship.

(23) Woodruff, W. H.; Margerum, D. W.; Milano, M. J.; Pardue, H. L.; Santini, R. E. *Inorg. Chem.* **1973**, *12*, 1490–1494.
(24) Woodruff, W. H.; Margerum, D. W. *Inorg. Chem.* **1974**, *13*, 2578–2585.
(25) Wajon, J. E.; Morris, J. C. *Inorg. Chem.* **1982**, 4258–4263.